

## Electric circuit analogy of heat losses of clothed walking human body in windy environment



Naghm Ismail<sup>a,b</sup>, Nesreen Ghaddar<sup>a,\*</sup>, Kamel Ghali<sup>a</sup>

<sup>a</sup> Mechanical Engineering Department, American University of Beirut, P.O. Box 11-0236, Beirut, 1107-2020, Lebanon

<sup>b</sup> Mechanical Engineering Department, Rafic Hariri University, P.O. Box 10, Damour-Chouf, 2010, Lebanon

### ARTICLE INFO

#### Keywords:

Clothed human heat loss

Electric circuit analogy

Clothing dynamic resistance

### ABSTRACT

In this study, a simplified approach for the estimation of the segmental heat losses from the human body to the environment is developed. The approach is based on a heat resistance model that predicts the latent and sensible heat losses while incorporating an analogy between the air flow and an electric circuit to determine the clothed limb or trunk segment ventilation induced by motion and wind. The estimation of the segmental ventilation allows the correction of the clothing dry/evaporative resistances in the heat resistance network to determine the dynamic resistance. The circuit models of heat and ventilation are validated by conducting experiments on a thermal manikin investigating the following cases: (i) no wind and no walking conditions (ii) wind (0.8 m/s) without walking condition (iii) walking (0.8 m/s) without wind (iv) wind (0.8 m/s) and walking (0.8 m/s) conditions. It was shown that the sensible heat loss segmental predictions of the circuit models were within the standard deviation range of the performed experiments.

The heat and ventilation circuit models are then integrated with a bio-heat model to calculate accurately the segmental skin temperature and sensible and latent heat losses from a clothed human under walking and wind conditions. The effect of ambient conditions on the latent and sensible heat losses and the effect of walking and wind speed on the thermal insulation are validated using available published experiments.

### 1. Introduction

Energy exchange between the human body and its thermal environment has been investigated by several researches interested in human thermal comfort in different applications including physiology, engineering, architecture, psychology and meteorology [1]. The quantification of the energy exchange between the human body and its environment is a complex task since any model developed for this purpose must find a balance between the physiological characteristics of the clothed human body and the environment conditions [2]. The heat exchange between human body and the environment is significantly influenced by the way the clothing layers mediate the flow of heat and moisture from the human skin to the environment. This exchange occurs either by diffusion in fabric and air layers or by ventilation induced by relative wind or walking condition resulting in air penetration through the fabric to microclimate air trapped between skin and fabric [3,4]. When human skin releases heat and moisture, some goes through clothing material, and the other is transferred from the microclimate air layer by ventilation. Since the clothing outer surface is exposed to the environment, conduction, convection and radiation

mechanisms help in heat transfer while diffusion, absorption, and evaporation mechanisms help in moisture transfer.

Researchers have modeled the thermal response of the clothed human body by either considering the clothing as static resistance [5] or by considering the dynamic properties of fabrics [6]. Recently, researchers reported that clothing ventilation at elevated speeds played a critical role in removing sensible and latent heat from the body to the environment [3,7]. Havenith et al. established that clothing ventilation can cause up to 50% reduction in thermal insulation and up to 88% reduction in evaporative resistance depending on the level of activity [8]. Therefore, modeling the heat and mass transfer of the clothed human body to environment necessitates the knowledge of the ventilation rate.

In order to predict the heat and moisture transfer from the human body, Lotens [9] developed a steady-state heat resistance network model that describes all the mechanisms of heat and moisture transfer from the skin to the environment. The network included all the mechanisms in addition to the dynamic resistance that takes into account the change in the dry and evaporative resistance due to clothing ventilation. The heat and moisture heat resistance network has then been

\* Corresponding author.

E-mail address: [farah@aub.edu.lb](mailto:farah@aub.edu.lb) (N. Ghaddar).

**Nomenclature**

|                         |   |
|-------------------------|---|
| $cp_a$                  | air specific heat (J/kg·K)  |
| $e_f$                   | thickness of the outer cylinder representing the fabric (m)                       |
| DSPM                    | double-steps per minute   |
| $f$                     | walking frequency (Hz)  |
| $f_{cl}$                | clothing area factor  |
| $H$                     | cylinder length (m)   |
| $R_{total}$             | total thermal insulation ((m <sup>2</sup> ·K/W)                                   |
| $I_I$                   | electric current (A)  |
| $L$                     | electric inductance   |
| $\dot{m}_{vent-radial}$ | ventilation rate through clothing (kg/m <sup>2</sup> ·s)                          |
| $\dot{m}_{vent-axial}$  | ventilation rate through opening (kg/m <sup>2</sup> ·s)                           |
| $P$                     | Pressure (Pa)   |
| $P_{skin}$              | skin water vapor pressure (Pa)  |
| $P_{env}$               | environment water vapor pressure (Pa)   |
| $P_{micro-air}$         | microclimate water vapor pressure (Pa)  |
| $P_{i-f}$               | inner fabric water vapor pressure (Pa)  |
| $P_{o-f}$               | outer fabric water vapor pressure (Pa)  |
| $Q$                     | Heat losses (W/m <sup>2</sup> )   |
| $R$                     | electric resistance   |
| $R_d$                   | dry thermal resistance (m <sup>2</sup> ·K/W)                                      |
| $R_{dynamic}$           | dynamic resistance (m <sup>2</sup> ·K/W)  |
| $R_{i-air}$             | inner cylinder convection resistance (m <sup>2</sup> ·K/W)                        |
| $R_{i-fabric}$          | inner fabric surface convection resistance (m <sup>2</sup> ·K/W)                  |
| $R_{i-rad}$             | radiative heat resistance between inner cylinder and fabric (m <sup>2</sup> ·K/W) |
| $R_{o-rad}$             | radiative heat resistance between outer cylinder and fabric (m <sup>2</sup> ·K/W) |
| $R_{o-env}$             | outer convective resistance to the environment (m <sup>2</sup> ·K/W)              |
| $R_{dynamic}$           | dynamic resistance (m <sup>2</sup> ·Pa/W)   |
| $Re_{dynamic}$          | evaporative dynamic resistance (m <sup>2</sup> ·Pa/W)                             |
| $Re_{i-air}$            | evaporative inner cylinder resistance (m <sup>2</sup> ·Pa/W)                      |
| $Re_{i-fabric}$         | evaporative inner fabric surface resistance (m <sup>2</sup> ·Pa/W)                |
| $Re_{o-env}$            | evaporative outer fabric resistance to the environment                            |

|                 |   |
|-----------------|---|
|                 | (m <sup>2</sup> ·Pa/W)  |
| $RH$            | relative humidity (%)   |
| $r_s$           | radius of the inner cylinder representing the human body skin (m) |
| $r_f$           | radius of the outer cylinder representing the fabric (m)          |
| $t$             | time (s)  |
| $T_{skin}$      | skin temperature (°C)   |
| $T_{env}$       | environment temperature (°C)                                      |
| $T_{micro-air}$ | microclimate air temperature (°C)                                 |
| $T_{i-f}$       | temperature of inner fabric (°C)                                  |
| $T_{o-f}$       | temperature of outer fabric (°C)                                  |
| $v_w$           | wind velocity (m/s)   |
| $v_{walk}$      | walking velocity (m/s)  |
| $y$             | radial direction  |
| $Y$             | microclimate air layer size (m)                                   |
| $\bar{Y}$       | average microclimate air layer size (m)                           |

**Greek symbols**

|              |  |
|--------------|--|
| $\Delta P_m$ | standard pressure difference (Pa)                          |
| $\mu$        | dynamic viscosity (kg/m·s)                                 |
| $\rho$       | density of air (kg/m <sup>3</sup> )                        |
| $\alpha$     | permeability of fabric (m <sup>3</sup> /m <sup>2</sup> ·s) |

**Subscripts**

|                  |   |
|------------------|---|
| <i>axial</i>     | axial direction                         |
| <i>angular</i>   | angular direction                       |
| <i>back</i>      | back side                               |
| <i>front</i>     | front side                              |
| <i>outside 1</i> | ambient side at the opening aperture    |
| <i>outside 2</i> | ambient side around the porous cylinder |
| <i>sens</i>      | sensible                                |
| <i>lat</i>       | latent                                  |

used in different studies to find the heat losses in different conditions. For example, Ghali et al. [10] incorporated the effect of ventilation induced by swinging motion of clothed cylinder in uniform wind to the Loten's simple heat resistance network model [9] to predict the mean steady periodic heat loss from the clothed cylinder. However, the used ventilation model was complex. It was based on solving the mass and momentum conservation equations inside the microclimate air layer between the skin and the clothing [11,12]. Furthermore, it took into account the effect of walking conditions by modeling the swinging motion of a clothed limb [3,10,13–15]. Although these mathematical models succeeded in predicting the segmental ventilation rates through clothing; however, they necessitated significant computational cost which made them difficult to be integrated with other thermal models to predict the segmental and overall heat losses. Consequently, Ismail et al. [16] developed a simplified model based on an analogy between the air flow inside the microclimate air layer and an electric circuit. This analogy circuit model predicted the segmental ventilation rate by using a resistance-inductance circuit. The electric resistance describes the resistance to the air flow while the electric inductance describes the resistance to the change in air flow rate if oscillation occurs. Their model, if coupled with the complex heat transfer circuit model, could be a start for changing research on clothing ventilation and comfort from empirical to effective, robust and simplified modeling approach.

Therefore, it is of interest to couple both heat resistance with ventilation circuit models to predict the segmental heat losses under different conditions. Because the heat resistance network model assumes a constant skin temperature, which is not the case in the real life scenario where the skin temperature depends on the metabolic rate and the

environment conditions and varies from one segment to the other, a bio-heat model is used [17]. The bio-heat human model is capable of predicting accurately human transient physiological responses such as the body's skin temperature is integrated with the circuit models of heat and ventilation. The effect of ambient conditions on the latent and sensible heat losses and the effect of walking and wind speed on the thermal insulation are investigated and validated using available published experiments [8,18].

**2. Methodology**

The research methodology consists of developing a simplified approach based on the steady-state resistance network model. Because the resistance network model depends significantly on the clothing ventilation which is critical in the removal of the sensible and latent losses, the prediction of the clothing ventilation is necessary. A simplified ventilation model based on an electric circuit analogy is adopted. Therefore, the methodology begins by describing the physical configuration of the problem that consists of a clothed cylinder representing the clothed human segment under different conditions. Afterwards, the steady state heat resistance network is described followed by a description of the ventilation electric circuit. The coupling between these two models is validated by conducting experiments on a thermal manikin at different wind conditions and body motion for a constant skin temperature. In order to find accurate segmental skin temperature, a bio-heat model is then coupled to the validated analogous electric circuit heat and ventilation models to accurately predict the human thermal response under a given metabolic rate that depends on the

activity level of the human body. The outputs of the integration with the bio-heat model are the segmental skin temperature, the segmental latent and sensible heat losses, the total thermal insulation. The integrated bio-heat and analogous electric circuit heat and ventilation models were then validated by comparing with available published experimental data. First, the sensible and latent heat losses are compared with the experiment of Fu [18] conducted on sedentary human subjects at different ambient conditions (relative humidity and temperature) in still air (no wind, no walking conditions). Second, the effect of walking and wind on the total thermal insulation is investigated and compared with the experimental results of Havenith et al. [8] using three different ensembles.

2.1. Physical configuration

Fig. 1 represents the clothed human body formed by clothed segment representing the clothed arm, trunk, or leg. Each clothed segment is represented by a fabric covered cylinder consisting of two concentric cylinders of inner radius  $r_s$ , outer radius  $r_f$ , and height  $H$ . The inner cylinder represents the human skin and is maintained at the skin temperature  $T_{skin}$ . The outer porous cylinder represents the isotropic fabric layer of permeability  $\alpha$  and thickness  $e_f$  considered as lumped layer of two fabric nodes (outer and inner) of different temperatures  $T_{o-f}$  and  $T_{i-f}$ . The physical configuration adopted has been extensively used in the literature to approach the clothed segment when estimating the ventilation [19–22] or when simulating the human thermal response [23–30]. The microclimate air annulus of thickness  $Y = r_f - r_s$  and temperature  $T_{micro-air}$  is trapped between the inner solid cylinder and the outer porous cylinder. The temperature and the pressure are considered constant over the height of the microclimate air layer. Indeed, the detailed model developed by Ismail et al. [12] shows that the variation of the pressure and temperature along the axial and angular direction does not exceed 6% and this allows to consider lumped conditions as the case of the radial direction. From here comes the validity of developing a simplified model that considers one pressure and temperature in the axial microclimate air layer direction. The fabric covered cylinder could be opened at the top or the bottom or closed at both ends. The heat transfer mechanism is shown in Fig. 1: the human

skin transfers heat to the environment by convection and radiation. The convection heat transfer is due to the motion of air in the microclimate air layer and outside in the environment. The motion of air inside the microclimate air layer is the result of the air renewal in the microclimate air layer (ventilation) either through clothing or through openings caused by walking and windy conditions.

2.2. Heat resistance network model

Fig. 2(a) shows the dry heat network of the ventilated clothed cylinder. The heat network includes the radiative heat exchange, the convective resistances due to the air motion inside the microclimate air layer and outside in the environment, the dynamic resistance which includes the dry resistance of the clothing corrected for radial ventilation of renewal air. When the aperture of the clothed cylinder is closed, the switch S is opened and vice versa. Indeed, the open aperture network differs from the closed aperture by the presence of additional heat exchange path between environment and microclimate air due to ventilation through opening. Fig. 2(b) represents the evaporative heat network of the ventilated clothed cylinder. The network includes the evaporative transfer resistances between the skin and the microclimate air layer, the air layer and the inner fabric surface, and between the outer fabric surface and the environment. Furthermore, the network includes the dynamic evaporative resistance that consists of the corrected evaporative resistance of clothing due to ventilation. Similarly to the dry heat network, the open aperture network differs from the closed aperture by the presence of additional mass exchange path between environment and microclimate air due to ventilation through opening.

The equations of the dry and evaporative resistances are obtained from expressions reported by Ghaddar et al. [19]. The dynamic dry and evaporative resistances are given by the following equations:

$$R_{dynamic} = \frac{1}{\left(\frac{1}{R_d + \dot{m}_{vent-radial} \times C P_a}\right)} \times \frac{r_s}{r_f} \tag{1a}$$

$$R_{e,dynamic} = \frac{1}{\left(\frac{1}{R_e} + \frac{1}{\rho \times R H_2 O \times T_{env} / \dot{m}_{vent-radial} \times h_{ad}}\right)} \times \frac{r_s}{r_f} \tag{1b}$$

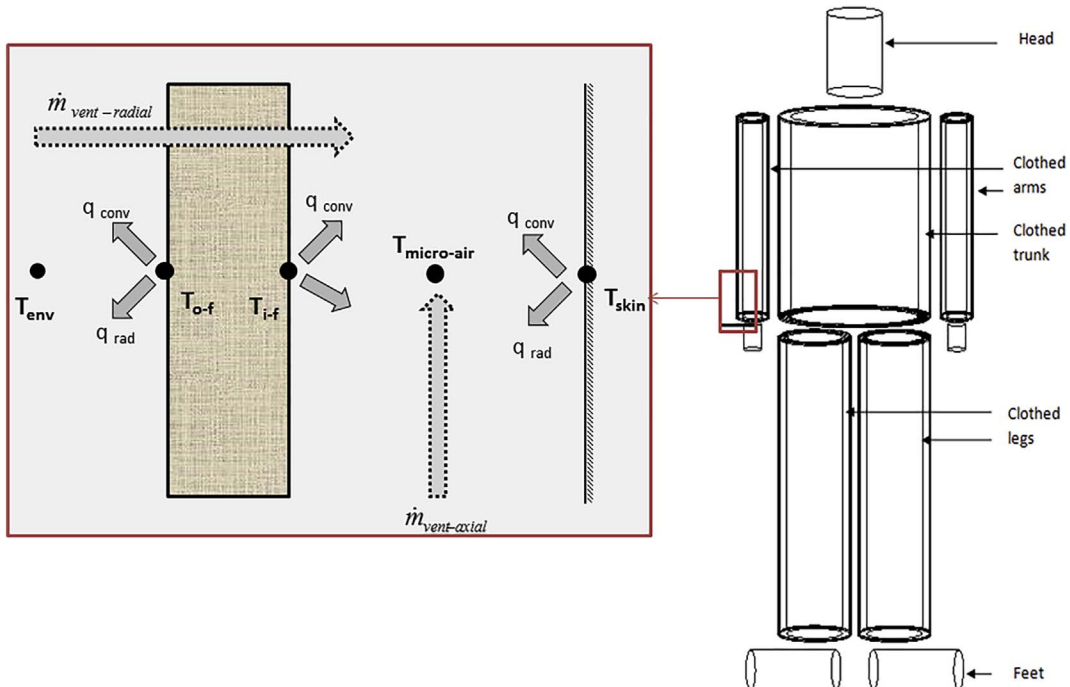
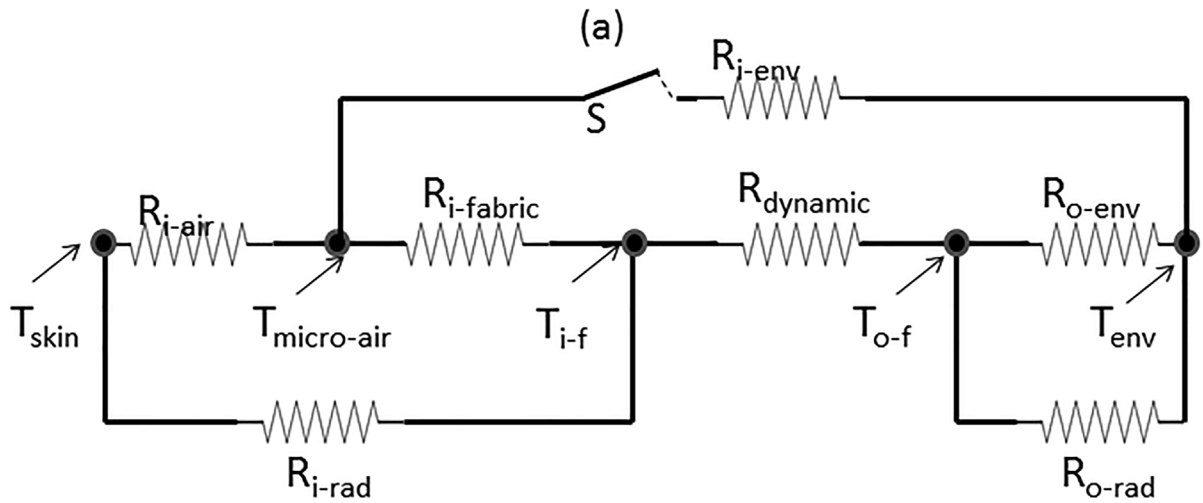
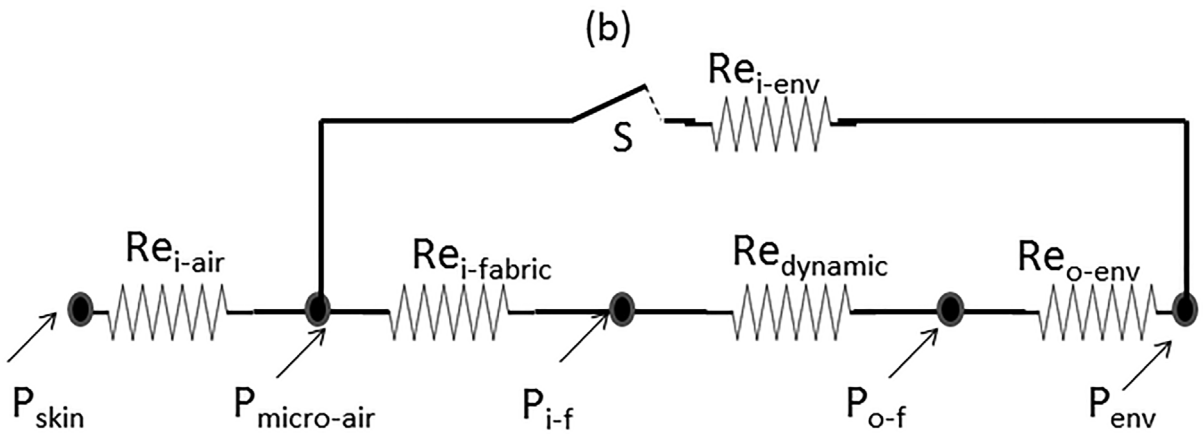


Fig. 1. Schematic of different mechanisms of heat transfer from the human body as well as the ventilation through clothing and openings.



|             |  |                |   |
|-------------|--|----------------|---|
| $R_{i-air}$ | Inner cylinder convection resistance                           | $R_{i-fabric}$ | Inner fabric surface convection resistance                                |
| $R_{i-rad}$ | Radiative heat resistance between inner cylinder and fabric    | $R_{dynamic}$  | Fabric dry resistance corrected by the dynamic resistance for ventilation |
| $R_{o-env}$ | Outer convective resistance to the environment                 | $R_{i-env}$    | Convective resistance to the environment through opening                  |
| $R_{o-rad}$ | Radiative heat resistance between outer fabric and environment |                |   |



|              |   |                 |   |
|--------------|---|-----------------|---|
| $Re_{i-air}$ | Inner cylinder evaporative resistance                     | $Re_{i-fabric}$ | Inner fabric surface evaporative resistance                                       |
| $Re_{o-env}$ | Outer evaporative resistance to the environment           | $Re_{dynamic}$  | Fabric evaporative resistance corrected by the dynamic resistance for ventilation |
| $Re_{i-env}$ | Evaporative resistance to the environment through opening |                 |   |

Fig. 2. Resistance network model of (a) dry heat and (b) evaporative heat.

where  $R_{dynamic}$ ,  $R_d$  and  $R_e$  are, respectively, the dynamic resistance for ventilation through clothing, the fabric dry resistance, and the fabric evaporative resistance,  $\dot{m}_{vent-radial}$  is the ventilation rate through clothing defined as the mass flow rate of air penetrating through  $1\text{ m}^2$  of the outer surface of the studied clothed segment ( $\text{kg}/\text{m}^2\cdot\text{s}$ ),  $C_{p_w}$ ,  $R_{H_2O}$ ,  $\rho_w$ ,  $h_{ad}$  are the specific heat, the water vapor gas constant, the air

density, and the fabric water vapor heat of adsorption; finally  $r_s$  and  $r_f$  are the skin and fabric cylinder radius.

Consequently, the segmental sensible and latent heat losses can be estimated based on the dry and evaporative resistance network respectively as follows:

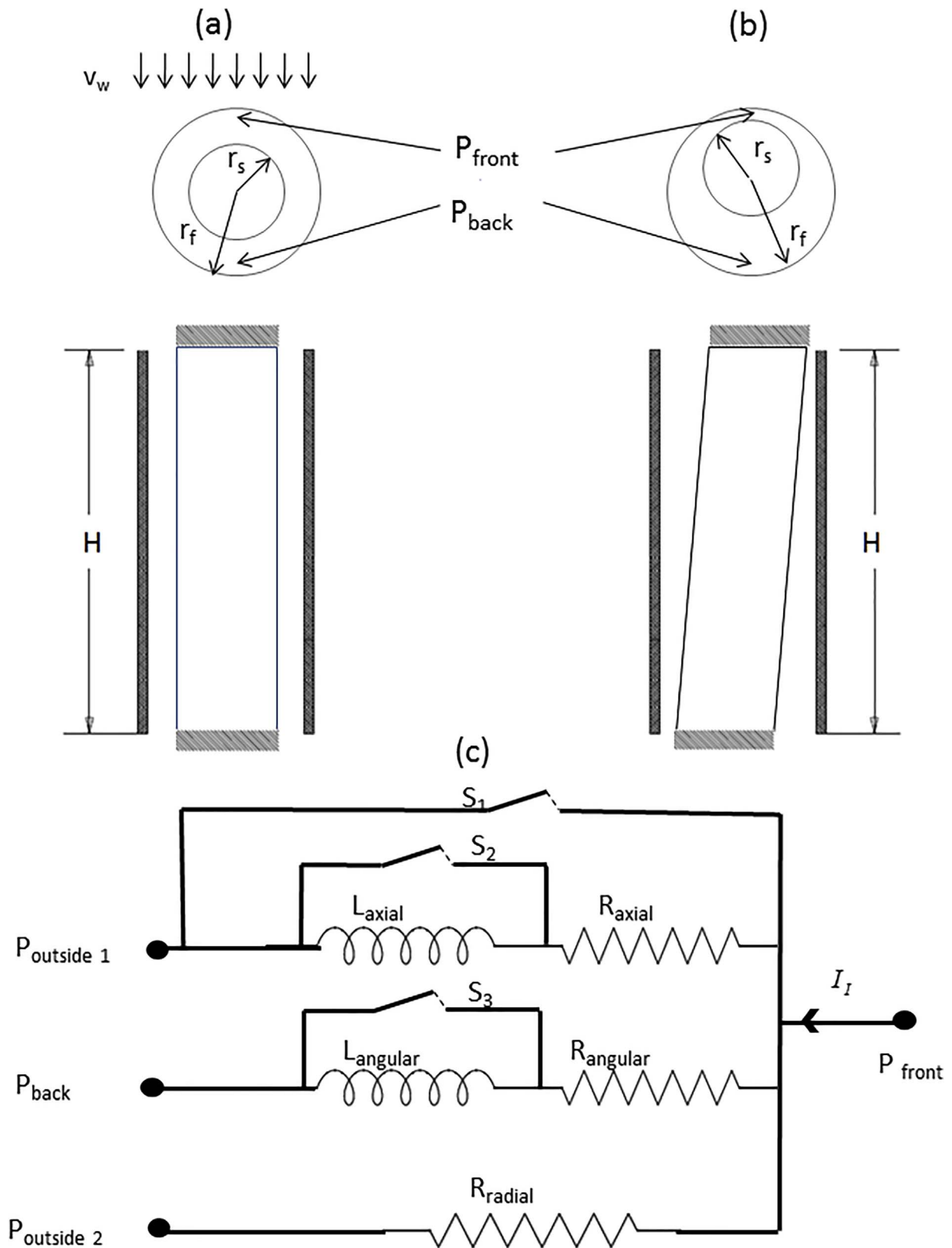


Fig. 3. Figure showing (a) the physical configuration of fabric clothed segment in windy conditions (b) the physical configuration of fabric clothed segment in oscillating motion and (c) the network representing the analogy of the air flow inside the microclimate air layer in oscillating motion where  $H$ ,  $r_s$  and  $r_f$  are the height, inner and outer radius respectively;  $P_{front}$  and  $P_{back}$  are the front and back pressures respectively and  $v_w$  is the wind speed;  $P_{outside1}$  and  $P_{outside2}$  are the pressures at the opening (if the aperture is opened at one end) and around the porous cylinder from the outside respectively.

$$Q_{sens} = \frac{(T_{skin} - T_{micro-air})}{R_{i-air}} + \frac{(T_{skin} - T_{i-f})}{R_{i-rad}} \quad (2a)$$

$$Q_{lat} = \frac{(P_{skin} - P_{micro-air})}{Re_{i-air}} \quad (2b)$$

### 2.3. Air flow resistance-inductance network model

The ventilation model of Ismail et al. [16] used the analogy of an electric circuit to estimate ventilation rates for the clothed segments and body postures (active or sedentary) at different windy conditions. The simplified model divided the fabric covered cylinder into two parts: one in front of the wind velocity if any and the other is on the back side. Therefore, each clothed segment had two pressures under investigation:  $P_{front}$  and  $P_{back}$  as shown in Fig. 3(a–b). Because the clothing ventilation is modeled as a pressure driven flow [3,10,15], the flow equations are converted to the equations of electric circuit where the pressure difference is analogous to the voltage difference while the air flow is similar to the electric current. The analogy is based on: (i) describing the resistance to air flow by an electric resistance (ii) describing the resistance to the change of the air layer volume by an **electric inductance**. Indeed, the air flow is hindered by the clothing fabric resistance which is a function of clothing air permeability. When the air penetrates through clothing, it flows in the microclimate annulus between the skin surface and the clothing in the angular and the axial directions. Within the microclimate where the air flow is laminar, it is resisted by a viscous action at the wall and inner fabric surfaces. The viscous resistances in both angular and axial directions and the clothing resistance in the radial direction are analogous to electric resistances given respectively by:

$$R_{axial} = \frac{12 \times \mu \times H}{Y^3 \times (\pi \times r_s)} \quad (3)$$

$$R_{angular} = \frac{12\mu \times (\pi \times r_s)}{Y^3 \times H} \quad (4)$$

$$R_{radial} = \frac{\Delta P_m}{\alpha \times \pi \times r_s \times H} \quad (5)$$

where  $r_s$ ,  $H$ ,  $Y$  are respectively the radius, the height, and the air gap width of the clothed segment that could be the arm, the trunk, or the legs,  $\mu$  is the air viscosity,  $\alpha$  is the air permeability of the fabric at the standard pressure  $\Delta P_m = 124.5$  Pa [31].

While above model of resistances is applicable for non-moving segment, the analogy for walking condition that induces the clothed arm to swing is changed by adding an inductance [16]. The human clothed arm can be assumed to have a sinusoidal up and down (swinging) motion. According to Ghaddar et al. [3], the oscillating motion of the clothed arm is divided to two phase: no-touch and touch phases. In Phase I, the human skin (inner cylinder) swings without touching the porous media (outer cylinder) while, in Phase II, the human skin and the clothing fabric is in contact and swing together. The swinging motion of the human skin before that the contact with the clothing fabric occurs, induces a change in the volume of air in axial and angular directions. Obviously, when the human skin is moving frontward, the air gaps size decreases in the front side and increases in the back side in both directions. The change of the volume of air is represented by an electric inductance given by:

$$L_{axial} = \frac{\rho \times H}{\bar{Y} \times (\pi \times r_s)} \quad (6)$$

$$L_{angular} = \frac{\rho \times (\pi \times r_s)}{\bar{Y} \times H} \quad (7)$$

where  $\bar{Y}$  is the average microclimate air layer size in axial and angular directions. Therefore, the analog electric circuit shown in Fig. 3(c) is composed of an electric resistance and inductance and is used to find

the ventilation rate for any clothed segment for different conditions where  $P_{front}$  and  $P_{back}$  are respectively the front and back pressures,  $P_{outside1}$  and  $P_{outside2}$  are the pressures at the opening (if the aperture is opened at one end) and around the porous cylinder from the outside respectively. However, the opening and closure of the switches depend on the clothed segment considered and on the working conditions investigated. If the clothed segment has an opening to the outside (on the collars or the cuff), the switch  $S_1$  is opened and closed otherwise. If the clothed segment does not experience any oscillation, the switches  $S_2$  and  $S_3$  are closed and the current  $I_l$  is null. Finally, when the clothed segment is under oscillation, the switches  $S_2$  and  $S_3$  are opened and the electric current  $I_l$  accounts for the change in the volume with respect to time as follows:

$$I_l = H \times r_s \times \frac{dY}{dt} \quad (8)$$

It is of interest to note that the clothed trunk does not experience any oscillation even in walking condition. The clothed trunk is only moving in the opposite direction of wind, therefore, the relative velocity increases by the walking velocity. In case of clothed leg, the ventilation rate is estimated based on the same strategy of the clothed trunk. The main reasons are: (i) the stance phase occupies 60% from the gait cycle; in this phase the clothed leg is vertical (ii) in the swing phase, the clothed leg is deployed: the thigh goes forward while the calf goes backward. Although the knee angle attains 60°; however, the increase in the relative wind speed of the thigh is compensated by the decrease of the relative wind speed of the calf. Based on these facts, the assumption of considering the same strategy of the clothed trunk in estimating the clothed leg ventilation is valid.

### 2.4. Integration with the bio-heat model

The developed approach of this study assumes a constant skin temperature of about 35 °C. However, in real life scenario, the skin temperature is not constant and depends on the metabolic rate, the body segment, the ambient conditions, and the clothing properties. Therefore, in order to find the accurate segmental skin temperature, a bio-heat model is coupled to the simplified heat and ventilation model. The bio-heat model used for this purpose divides the body into cylindrical segments [17]. Each body segment is composed of four nodes of core, skin, artery blood, and vein blood. The nude body model is integrated to an existing clothing model based on heat and mass diffusion through the clothing layers. The bio-heat human model is capable of predicting accurately human transient physiological responses such as the body's skin temperature and is validated in previous study reporting experiments performed at different conditions in a controlled environment [17]. The inputs of the bio-heat model are the ambient conditions, the clothing properties and the metabolic rate. The metabolic rate depends on the activity level. For instance, the metabolic rate for a standing human body used is 1.2 Met, while the metabolic rate for a walking human body at 0.8 m/s walking speed or 38 DSPM is 1.8 MET [32]. Although the simplified ventilation model does not consider the water vapor transport, the bio-heat model could be integrated with the simplified ventilation model because the water vapor transport does not affect the ventilation model significantly [20]. The coupling occurs by means of the dry and evaporative dynamic resistance that illustrates the change of clothing insulation due to ventilation and air movement [12]. The outputs of the integration with the bio-heat model are the segmental skin temperature, the segmental heat losses (sensible and latent) and the total thermal insulation affected by posture, movement, and wind defined by the following equation:

$$R_{total} = \frac{\bar{T}_{skin} - T_{env}}{\bar{Q}_{sens}} \quad (9)$$

where  $\bar{T}_{skin}$  and  $\bar{Q}_{sens}$  are respectively the area weighted average skin temperature and sensible heat losses. The validation of the integration

with the bio-heat model is achieved by comparing the outputs with the available published experiments on human subjects [8,18].

2.5. Experimental methodology using thermal manikin

The aim of the experiment is to validate the approach developed to estimate the segmental heat losses of clothed human body under different conditions for an isothermal skin temperature. The experiment was conducted using a 20-zone Newton thermal manikin [33] with zones shown in Fig. 4 and the actual manikin shown in Fig. 5 where the surface temperature or heating power of each body segment of the manikin could be controlled individually. Wire sensors were embedded in all the thermal zones to provide the requested skin temperature or heat flux with a standard deviation less than 0.01 °C. The thermal manikin can be controlled to have constant segmental skin temperatures in a constant skin temperature mode or constant segmental heating power in a constant heating power or heating flux mode. The heat flux generated and associated surface temperatures were recorded during experiments by ThermDAC® software exclusive for the thermal manikin on a separate computer.

As for the clothing, the manikin was clothed with a long sleeved cotton shirt and trousers having the properties illustrated in Table 1. The air permeability of the shirt and pants were measured by SDL MO2IA air permeability tester with a standard deviation in repeated measurements of  $\pm 10^{-4}$  and accuracy of  $0.1 l/(m^2 \cdot s)$ . The dry and evaporative resistances were measured using the sweating guarded hotplate (Model 306–200/400) with an error less than 0.1%. The openings are at the neck and the cuff level. The manikin is clothed by a belt to insure that there is no opening at waist line.

Three large fans with a diameter of 0.5 m were installed vertically

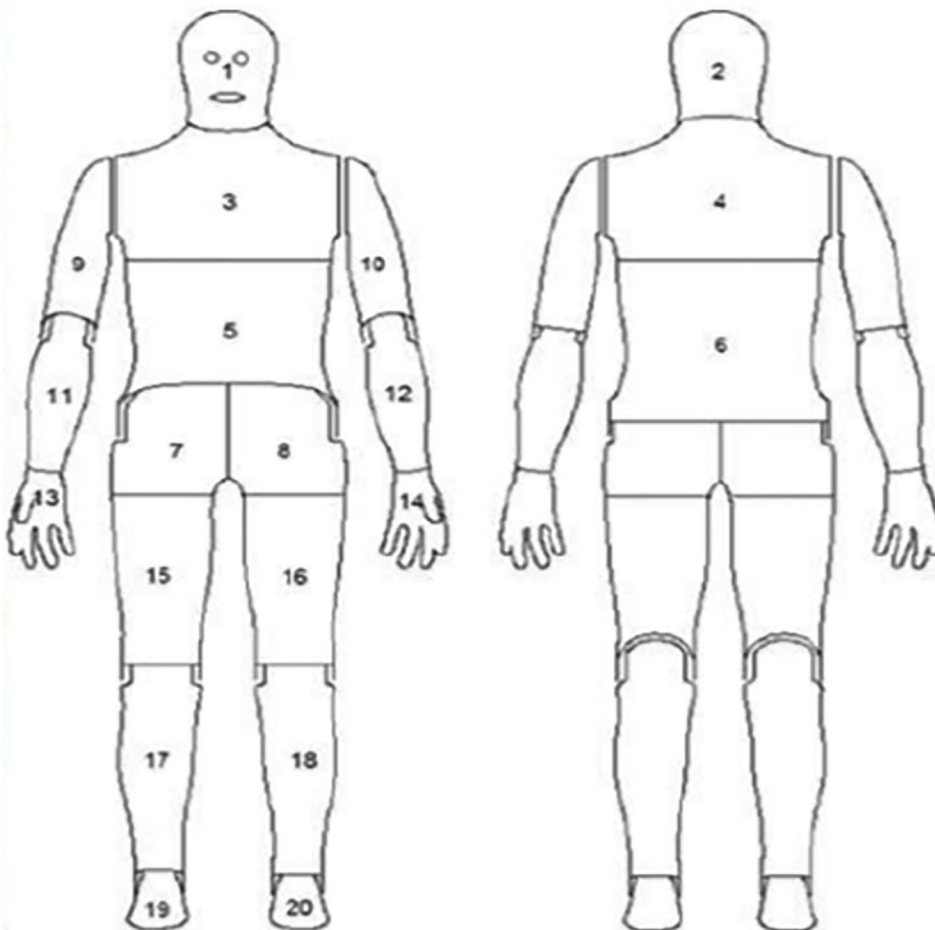
on a movable wooden stand. An air velocity transducer (model 8475–06) of  $\pm 3.0\%$  accuracy and a selective range of [0.05, 2.5 m/s] was used in the experiment. The transducer measured the distribution of wind speed at 3-min intervals at twelve locations (four in front of the upper chest at height 1.6 m from the floor, four in front of the lower chest at height 1.4 m from the floor, two in front of right and left thigh at height 1 m from the floor, and two in front of right and left calves at height 0.5 m from the floor) at a distance of 0.35 m from the manikin surface. The reported wind speeds were averaged and a mean value of wind speed was determined. It has been proven that the fan provides symmetrical distribution of the air velocity in front of the thermal manikin and uniform distribution along the height (z axis) with a maximum relative error of 6% [12]. The fans were switched off in no-windy condition ( $0.11 \text{ m/s} \pm 0.0066 \text{ m/s}$ ). In windy condition, the fans' stand was moved to where the wind speed measured by the manikin speed sensor was about  $0.8 \pm 0.048 \text{ m/s}$ .

In order to mimic the walking condition, Newton manikin was designed to generate smooth and realistic walking movement. Newton walking motion system contains a roll-around stand with integrated winch to help lifting, positioning, and transporting the manikin. In addition, it contains a motor, a drive assembly, and a quick-connect actuator rods needed to generate a walking motion. The walking speed was indicated manually using a motion control enclosure where it was continuously variable up to 60 double-steps per minute (DSPM).

The manikin, the fans and the walking stand were placed in an environmental chamber. The chamber air temperature was measured by two manikin sensors at different heights (0.9 m and 1.6 m) and the average was about  $25.5 \text{ °C} \pm 0.2 \text{ °C}$ . The relative humidity was measured at 1.6 m height and it was about  $60 \pm 3\%$ .

After setting the experimental ambient conditions (wind speed, air

Fig. 4. Figure showing the 20 zones of the thermal manikin used in the experiment [33].





(a)



(b)

Fig. 5. Experimental set up showing (a) thermal manikin walking (b) thermal manikin under windy condition.

**Table 1**  
Properties of the clothing ensemble.

|       | Material                    | Air permeability (m/s) | Dry resistance (K·m <sup>2</sup> /W) | Evaporative resistance (Pa·m <sup>2</sup> /W) |
|-------|-----------------------------|------------------------|--------------------------------------|---|
| Shirt | 100% cotton                 | 1.38                   | 0.046                                | 0.0044  |
| Pants | 75% cotton<br>25% polyester | 0.25                   | 0.041                                | 0.0065  |

temperature, and relative humidity), the thermal manikin was turned on and initialized to be at the thermo-neutral state. The manikin segmental skin temperatures were checked for thermal equilibrium with the room conditions to reach about 35 °C. Once equilibrium was reached, the manikin was tested at constant skin temperature set in ThermDAC<sup>®</sup> software. If the walking condition was considered, the walking speed was indicated manually. The duration of the experiment to reach steady state depended on the working conditions. The shortest experiment corresponded to the case of no walking and no windy conditions (30min), while the longest corresponded to the case of walking and windy conditions (70 min).

### 3. Results and discussions

#### 3.1. Experimental validation of the integrated model using the thermal manikin

In this section, a comparison is done between the sensible heat losses of the experiment conducted on the thermal manikin and those predicted by the integrated simplified model for the segmental heat losses. Although the thermal manikin could be used to test the latent heat exchange, however, this necessitates more involved experiment

**Table 2**  
The clothed segments area used in the current model.

| Segments                       | Chest | Back | Abdomen | Buttocks | Upper arm | Lower arm | Thigh | Calves |
|--------------------------------|-------|------|---------|----------|-----------|-----------|-------|--------|
| Surface Area (m <sup>2</sup> ) | 0.12  | 0.24 | 0.12    | 0.05     | 0.13      | 0.1       | 0.24  | 0.21   |

that requires additional equipment for a sweating skin. On the other hand, it has been shown in the literature that the sensible heat exchange is the most influenced by the ventilation through clothing [20]. Therefore, only sensible heat losses have been measured and compared to the model findings. Different conditions have been taken into account: (i) no wind and no walking conditions (ii) wind (0.8 m/s) without walking condition (iii) walking (38 DSPM or 0.8 m/s) without wind (iv) wind (0.8 m/s) and walking (38 DSPM or 0.8 m/s) conditions.

The inputs to the integrated simplified model are the clothing air permeability, the geometrical parameters of the clothed segments, and the oscillation parameters. In the simplified ventilation model, the clothed segments are the clothed trunk (associating the abdomen, the back, and the chest), the clothed arm (associating upper and lower arm), and the clothed leg (associating buttocks, thigh and calf). This is not the case in the bio-heat model where the human body is divided into several segments such as the chest, back, abdomen, upper and lower arm, thigh and calves. Therefore, once the bio-heat is integrated with the ventilation model, the ventilation predicted per m<sup>2</sup> area of the trunk will be incorporated to the chest, back, and abdomen to find the heat losses of such segments. In the same manner, the ventilation predicted for the clothed arm per m<sup>2</sup> area of the arm will be incorporated to the upper and lower arms to find the heat losses of such segments. The same method is used in the case of the legs divided into thigh and calves. The height, radius, and air gap of the clothed arm are respectively 58 cm, 3.8 cm, and 1.6 cm. The clothed arm end is opened at the bottom. The height, radius, and air gap of the clothed leg are respectively 95 cm, 7 cm, and 4 cm. The clothed leg end is opened at the bottom. The height, radius, and air gap of the clothed trunk are respectively 48 cm, 14 cm, and 5 cm. The clothed trunk is opened at the top end. These geometrical parameters are got from the clothed thermal manikin by averaging the geometrical parameters of (i) abdomen, back, and chest (ii) upper and lower arm (iii) buttocks, thigh and calf to find the geometrical parameters of the trunk, the arm and the leg respectively. The outer surface areas of each clothed segment is presented in

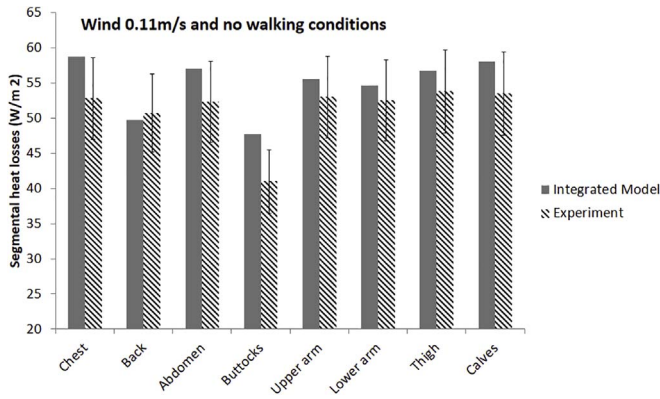


Fig. 6. Comparison between the measured and the predicted segmental heat losses for no windy and no walking conditions.

**Table 2.** For each simulation, the ventilation model took almost 400 iterations to converge during less than 2 min while it took approximately 25 min after the integration with a bio-heat model using Matlab R2014a software installed in a Lenovo H50 lab computer (Core i7, 8 GB RAM, 1 TB HDD) 90B7000JUS.

Fig. 6 shows the comparison between the measured and the predicted sensible segmental heat losses for the case of no wind and no walking condition. It is worth to mention that the thermal manikin velocity transducer indicated a wind speed of 0.11 m/s in the case of no wind (the fans are turned off). This velocity belongs to the air speed in a still air room; therefore, this value is used in the simulation to predict the ventilation rate and the dynamic resistance. The results show an agreement between the measured and the predicted segmental heat losses where all the predicted values fall within the standard deviation of the measured values. The maximum relative error is 16% at the buttocks level. The over-estimation of the simplified model of the buttocks segment could be related to the fact that in the experiment, the part of the shirt (under the pants) covered a part of buttocks. Thus, the buttocks' segment is enclosed by the shirt and the pants which increased the thermal resistance and then decreased the segmental heat losses in the experiment to be smaller than that used in the integrated model which is only the pants thermal resistance. On the other hand, it was shown that the largest heat losses are those of the lower human body parts (buttocks, thigh, and calves) compared to the upper human body parts (chest, back, and abdomen, upper and lower arm). This is due to the thermal resistance of clothing used in the upper human body parts greater by 13% 12% than that used for the lower human body parts.

Fig. 7 shows the comparison between the measured and the predicted segmental heat losses for the case of wind (0.8 m/s) without walking condition. All the predicted segmental heat losses fall within the standard deviation of the experimental results except for the buttocks for the same reason discussed in the first case. The segmental heat losses are obviously larger in the windy condition case than that when no wind exists. This is obviously due to the large ventilation rate induced by the flow of air through clothing and through openings. Another important remark is that in this case, the largest heat losses are those of the upper human body parts (chest, back, and abdomen, upper and lower arm) compared to the lower human body parts (buttocks, thigh, and calves). The main reason is that the upper human body is clothed with high air permeability shirt that induces more ventilation rate. The higher is the ventilation rate the higher is the destruction of the thermal resistance (equation (1 a)). Therefore, although the thermal resistance of the shirt is higher than that of pants, the dynamic resistance of the shirt is lower than that of pants (because of the high air permeability of the shirt) leading to higher heat losses.

Fig. 8 shows comparison between the measured and the predicted segmental heat losses for the case of no wind and walking condition ((38 DSPM or 0.8 m/s). It is worth to mention that in this case, the

thermal manikin does not simulate the human body motion. Indeed, the chest, the abdomen and the back are all moving at the walking speed (0.8 m/s) in the real case scenario which is not the case for the thermal manikin that only mimics the walking motion by oscillating the limbs. The forward motion of the chest, the abdomen, and the back at the walking speed could be compensated by exposing them to air at a speed equal to the walking speed. Moreover, the frequency  $f$  used for the oscillatory clothed arm is the same as the DSPM (double steps per minute) which is 38 rpm. For these inputs, the results show good agreement between the integrated simplified model and the experiment with a maximum relative error of 12% at the buttocks segment. On the other hand, it is shown that the segmental heat losses for the chest, the abdomen, and the back in the case of walking without wind are the same for the case of wind without walking. Indeed, as mentioned before, the motion of the chest, the abdomen and the back at a specified walking speed creates a relative velocity equals to the case of a chest at rest exposed to the same wind speed. As for the clothed arms, the segmental heat losses of the oscillating arm in no windy condition are greater by about 10% compared to the first case (no wind, no walking) and smaller by about 12% compared to the case of wind condition (0.8 m/s) without walking. The main reason is that the swinging motion of the clothed arm induces the air to enter and leave because of the change of the microclimate air layer size. This flow of air increases the ventilation rate through clothing and through openings and decreases the thermal resistance and thus increases the segmental heat losses. However, the segmental heat losses in the case of walking (0.8 m/s) without wind are smaller compared to the windy case without walking because the ventilation due to the presence of wind is greater than that of oscillatory motion [12]. The clothed legs show approximately the same heat losses in the case of walking (0.8 m/s) without wind compared to the windy case without walking (0.8 m/s). The reason is that the increase in the relative wind speed of the thigh is compensated by the decrease of the relative wind speed of the calf and vice versa. The agreement between the experiment and the integrated model for the clothed legs show that the assumption of adopting the same strategy of the clothed trunk when estimating the clothed leg ventilation is valid.

Fig. 9 shows comparison between the measured and the predicted segmental heat losses for the case of wind (0.8 m/s) and walking condition ((38 DSPM or 0.8 m/s). Good agreement is shown between the measured and the predicted heat losses. The maximum relative error is about 15% on the buttocks level. This case presents the maximum segmental heat losses compared to all other cases. The main reason is clearly the maximum ventilation rate induced when both wind and walking conditions are presented.

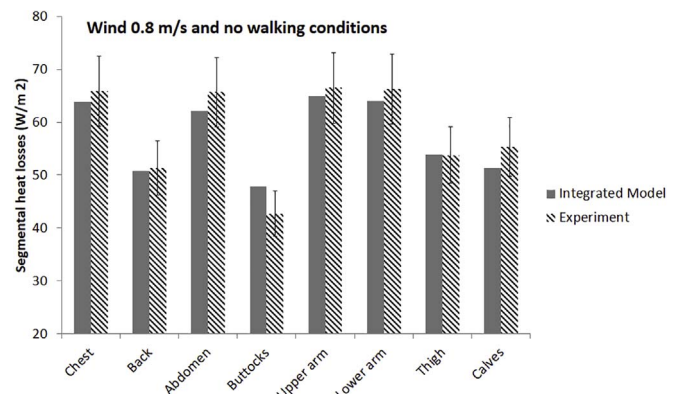


Fig. 7. Comparison between the measured and the predicted segmental heat losses for windy condition (0.8 m/s) and no walking condition.

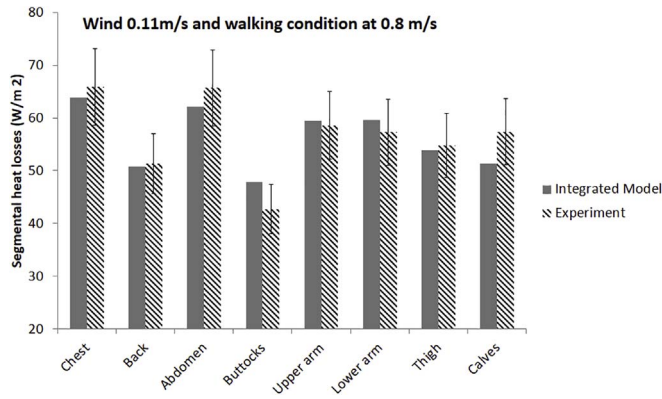


Fig. 8. Comparison between the measured and the predicted segmental heat losses for no windy condition and walking condition (0.8 m/s).

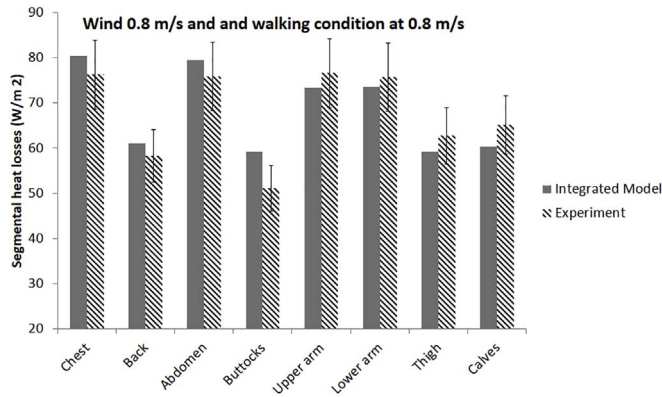


Fig. 9. Comparison between the measured and the predicted segmental heat losses for windy (0.8 m/s) and walking conditions (0.8 m/s).

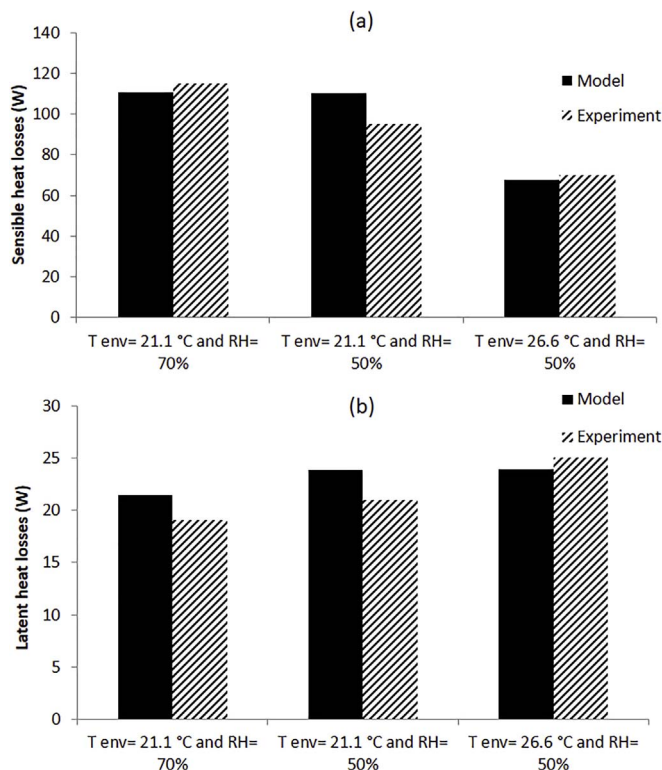


Fig. 10. Comparison between the predicted and the experimental (a) sensible heat losses and (b) latent heat losses.

### 3.2. Comparison with literature

#### 3.2.1. Effect of ambient temperature and relative humidity on latent and sensible heat losses

In this section, the simplified integrated model of heat and ventilation is used to find the sensible and latent heat losses for different ambient conditions and to compare these findings with the published experiments of Fu [18] who conducted different experiments on human subjects for different ambient conditions. The input parameters are all extracted from the study of Fu [18]. The metabolic rate used was 1 Met (Metabolic Equivalent for Task) and no wind conditions at 0.11 m/s were taken into account. As for the clothing ensemble, it was a sweat suit including briefs (100% cotton), long sleeve sweat suit (50% cotton, 50% polyester), sweat pants (50% cotton, 50% polyester), socks (100% cotton), and shoes (woven fabric, vinyl, knit). The environment temperature varied between 21 and 26 °C and the relative humidity between 50 and 70%. However, Fu [18] reported the total sensible and latent heat losses and not the segmental heat losses.

Fig. 10 shows the comparison between the total heat and latent heat losses for different conditions between the simulations achieved on the integrated model and the experiments conducted by Fu [18]. It is of interest to note that the total heat losses is estimated by summing the segmental heat losses shown in Table 3 while doubling the upper arm, lower arm, thighs, calves, hands and feet's segmental heat losses. Good agreement is shown between the estimated and the experimental heat losses with a mean relative error of about 6% and a maximum relative error of 15%. Examining Table 3, the effect of temperature change and the relative humidity on the predicted segmental sensible and latent heat losses can be analyzed. As the ambient temperature increased by 23%, all the sensible heat losses decreased by 43% while the latent heat losses decreased by 8%. The decrease in sensible heat losses is evidently related to the decrease in the temperature difference between the human body and the skin. On the other hand, the decrease in the latent heat losses is due to the increase in the environment vapor pressure when the temperature increases at the same relative humidity leading to a decrease in the vapor pressure difference between the human skin and the environment. When the relative humidity decreases, the segmental sensible heat losses does not show a significant change; however, the latent heat losses increase substantially: a decrease to the half of relative humidity leads to 40% increase approximately. It is also of interest to state that the latent heat losses of each segment, as shown in Table 3, is not significant compared to sensible heat losses. This is due to the small difference of partial pressure between the microclimate air layer and the environment where the partial pressure of air at the environment conditions ranges between 1251 Pa to 1752 Pa while the microclimate water vapor pressure is only differing by a range of 0.3–0.6%.

#### 3.2.2. Effect of wind and walking conditions on thermal insulation

In this section, a comparison between the integrated model results and the published experiments regarding the effect of the movement and wind on the total thermal insulation is achieved. The published experiments used are that of Havenith et al. [8] who conducted experiments on human subjects at several wind and walking conditions for different ensembles. The following three clothing ensembles were selected similar to ensembles used by Havenith et al. [8] in their experimental studies:

- (1) Ensemble A (permeable): workpants (cotton,  $\alpha = 0.212$  m/s,  $Rd = 0.092$  m<sup>2</sup>. K/W,  $Re = 0.0161$  m<sup>2</sup>. Pa/W), poly-shirt (50% polyester, 50% cotton,  $\alpha = 2.172$  m/s,  $Rd = 0.085$  m<sup>2</sup>. K/W,  $Re = 0.0081$  m<sup>2</sup>. Pa/W), and sweater (cotton, acrylic,  $\alpha = 1.622$  m/s,  $Rd = 0.07$  m<sup>2</sup>. K/W,  $Re = 0.0076$  m<sup>2</sup>. Pa/W).
- (2) Ensemble B (semi-permeable): ensemble A + a coverall (cotton,  $\alpha = 0.216$  m/s,  $Rd = 0.092$  m<sup>2</sup>. K/W,  $Re = 0.0161$  m<sup>2</sup>. Pa/W).
- (3) Ensemble C (impermeable): ensemble B + a rain coverall (nylon,

**Table 3**  
Segmental sensible and latent heat losses for different ambient conditions.

| Segments  | Heat losses (W) | T <sub>env</sub> = 21.1 °C and RH = 70% | T <sub>env</sub> = 21.1 °C and RH = 50% | T <sub>env</sub> = 26.6 °C and RH = 50% |
|-----------|-----------------|---|---|---|
| Chest     | sensible        | 4.39                                    | 4.40                                    | 2.54                                    |
|           | latent          | 1.71                                    | 1.93                                    | 1.78                                    |
| Back      | sensible        | 3.74                                    | 3.73                                    | 2.16                                    |
|           | latent          | 1.54                                    | 1.73                                    | 1.60                                    |
| Abdomen   | sensible        | 2.61                                    | 2.61                                    | 1.56                                    |
|           | latent          | 1.04                                    | 1.18                                    | 1.08                                    |
| Buttocks  | sensible        | 2.83                                    | 2.83                                    | 1.70                                    |
|           | latent          | 0.12                                    | 0.28                                    | 0.17                                    |
| Upper arm | sensible        | 5.59                                    | 5.58                                    | 3.21                                    |
|           | latent          | 1.65                                    | 1.88                                    | 1.74                                    |
| Lower arm | sensible        | 3.96                                    | 3.95                                    | 2.27                                    |
|           | latent          | 1.65                                    | 1.17                                    | 1.09                                    |
| Thigh     | sensible        | 15.22                                   | 15.16                                   | 8.78                                    |
|           | latent          | 2.00                                    | 2.47                                    | 3.25                                    |
| Calves    | sensible        | 9.32                                    | 9.25                                    | 5.36                                    |
|           | latent          | 1.93                                    | 2.27                                    | 2.11                                    |
| Head      | sensible        | 11.79                                   | 11.70                                   | 11.42                                   |
|           | latent          | 1.12                                    | 1.34                                    | 1.25                                    |
| Hands     | sensible        | 8.02                                    | 7.96                                    | 4.31                                    |
|           | latent          | 0.70                                    | 0.82                                    | 0.77                                    |
| Feet      | sensible        | 0.52                                    | 0.49                                    | 0.24                                    |
|           | latent          | 0.03                                    | 0.05                                    | 0.07                                    |

**Table 4**  
Effect of walking and wind conditions on thermal insulation  $R_{total}$  (m<sup>2</sup>K/W) for different ensembles and % reduction in value compared to base case of 0 walking speed and no wind.

| Case           | $v_{walk}$ (m/s) | $v_w$ (m/s) | $R_{total}$ (m <sup>2</sup> K/W) [% reduction in total dry insulation] |            |            |            |
|----------------|------------------|-------------|--|------------|------------|------------|
|                |                  |             | Ensemble A   | Ensemble B | Ensemble C |            |
| Reference case | 0                | 0           | 0.19   | 0.23       | 0.25       |            |
| Wind only case | 0                | 0.7         | 0.16 [16%]   | 0.17 [26%] | 0.20 [20%] |            |
|                | 0                | 4.1         | 0.12 [37%]   | 0.14 [39%] | 0.15 [40%] |            |
| Walking cases  | 0.3              | 0           | 0.16 [16%]   | 0.21 [9%]  | 0.21 [16%] |            |
|                | without and      | 0.3         | 0.7  | 0.14 [26%] | 0.17 [26%] | 0.17 [32%] |
|                |                  | 0.3         | 4.1  | 0.11 [42%] | 0.13 [43%] | 0.14 [44%] |
|                | with wind        | 0.9         | 0  | 0.15 [21%] | 0.16 [30%] | 0.17 [32%] |
|                |                  | 0.9         | 0.7  | 0.13 [32%] | 0.14 [39%] | 0.14 [44%] |
|                |                  | 0.9         | 4.1  | 0.09 [53%] | 0.11 [52%] | 0.11 [56%] |

$$\alpha < 0.005 \text{ m/s}, Rd = 0.013 \text{ m}^2 \cdot \text{K/W}, Re = 0.0007 \text{ m}^2 \cdot \text{Pa/W}.$$

In all these ensembles, the human trunk is assumed to have an inner underwear thin cotton liner layer with a very small dry resistance such that the skin temperature and inner layer temperature differ by less than 0.05 °C. Different posture/movement types were simulated; standing, and walking at two speeds: 0.3 m/s and 0.9 m/s. In addition, three wind conditions were tested: no wind ( $v_w < 0.1$  m/s), 0.7 m/s, and 4.1 m/s. The ambient conditions tested are:  $T_{env} = 23$  °C and  $RH = 50\%$ .

The simulation of the integrated model began by calculating the ventilation rate from the simplified ventilation model. Therefore, the clothing permeability of each segment was set for each ensemble case. When the clothed segment was covered by different layers, the lowest permeability is used. The windy and walking conditions were also defined in the simplified ventilation model and the segmental ventilation rates were estimated. The metabolic rate corresponding to each activity level as well as the ambient conditions were set in the bio-heat model. As for clothing, the thermal and evaporative resistances of each ensemble are set properly. Afterwards, the segmental skin temperature and the heat losses were averaged and the thermal insulations for different conditions were estimated.

Table 4 summarizes the resulting total insulation for the simulated

cases. It is observed that the total insulation was reduced from the reference value (no walking, no wind) by 8–16% when walking at 0.3 m/s and by 21–32% when walking at 0.9 m/s. In windy conditions, the total insulation was reduced by 15–26% at wind speed of 0.7 m/s and by 36–40% at wind speed of 4.1 m/s. When combining postures/movements with wind a reduction up to 56% is observed. These findings agree with the findings of Havenith et al. [8] who conducted experiments on human subjects at the same wind and walking conditions for the same ensembles and reported similar reductions in total insulation of the ensembles (11–15% reduction in walking at 0.3 m/s; 18–32% reduction in walking at 0.9 m/s; 15–26% reduction in wind at 0.7 m/s; 34–40% reduction in wind at 4 m/s; and up to 53% reduction in combined wind and walking).

#### 4. Conclusion

A new approach is developed to find the segmental heat losses from the human body to the environment. The approach is based on integrating a simplified ventilation model that is based on a simple electric analogy with a heat resistance network. The integration is established by means of the dynamic resistance where the dry resistance is corrected to account for the segmental ventilation rate. The predictions of the integrated model is compared to the results of an experiment conducted on a thermal manikin at different conditions: no walking and no wind conditions, walking without wind conditions, wind without walking conditions, and wind with walking conditions. All the predictions fall into the standard deviation of the experiment where the maximum relative error is about 16%. The maximum segmental heat losses occur in the case of wind and walking conditions followed by the case of windy condition. In order to find the segmental skin temperature, the simplified ventilation model is integrated with a bio-heat model that simulates the human thermal response by correcting for the dynamic resistance and setting the corresponding metabolic rate. It is shown that the total insulation was reduced from the reference value (no walking, no wind) by 8–16% when walking at 0.3 m/s and by 21–32% when walking at 0.9 m/s. Furthermore, the total insulation was reduced in windy conditions by 15–26% at wind speed of 0.7 m/s and by 36–40% at wind speed of 4.1 m/s. Finally, when combining postures/movements with wind a reduction of the thermal insulation up to 56% is observed. The developed simplified model can be used as an interactive optimization design tool in different clothing design applications for sports and warm climates by finding the heat losses and ventilation rates associated with the type of clothing without the need to run complex models or conducting experiments.

#### Acknowledgement

We would like to acknowledge the financial support of the Lebanese National Council for Scientific Research for the project Award Number103061-22909.

#### References

- [1] R.J.D. Dear, E. Arens, Z. Hui, M. Oguro, Convective and radiative heat transfer coefficients for individual human body segments, *Int J Biometeorol* 40 (1997) 141–156, <http://dx.doi.org/10.1007/s004840050035>.
- [2] C.A. U' Mander, E. Brebbia, F. Tiezzi, V. Gomez, L. Sifre, *Monyero, Sustainability in cities: the green areas and climatic comfort as fundamental parameters, The Sustainable City IV: urban regeneration and sustainability*, WIT, Southampton, 2006, pp. 83–94.
- [3] N. Ghaddar, K. Ghali, B. eije Jr., Ventilation of wind-permeable clothed cylinder subject to periodic swinging motion: modeling and experimentation, *J Heat Tran* 130 (2008) 091702, <http://dx.doi.org/10.1115/1.2944245>.
- [4] X. Wan, J. Fan, A transient thermal model of the human body—clothing—environment system, *J Therm Biol* 33 (2008) 87–97, <http://dx.doi.org/10.1016/j.jtherbio.2007.11.002>.
- [5] S.-I. Tanabe, K. Kobayashi, J. Nakano, Y. Ozeki, M. Konishi, Evaluation of thermal comfort using combined multi-node thermoregulation (65MN) and radiation models and computational fluid dynamics (CFD), *Energy Build* 34 (2002) 637–646,

- [http://dx.doi.org/10.1016/s0378-7788\(02\)00014-2](http://dx.doi.org/10.1016/s0378-7788(02)00014-2).
- [6] L. Yi, L. Fengzhi, L. Yingxi, L. Zhongxuan, An integrated model for simulating interactive thermal processes in human–clothing system, *J Therm Biol* 29 (2004) 567–575, <http://dx.doi.org/10.1016/j.jtherbio.2004.08.071>.
- [7] X.-Q. Dai, R. Imamura, G.-L. Liu, F.-P. Zhou, Effect of moisture transport on microclimate under T-shirts, *Eur J Appl Physiol* 104 (2007) 337–340, <http://dx.doi.org/10.1007/s00421-007-0628-z>.
- [8] G. Havenith, R. Heus, W.A. Lotens, Resultant clothing insulation: a function of body movement, posture, wind, clothing fit and ensemble thickness, *Ergonomics* 33 (1990) 67–84, <http://dx.doi.org/10.1080/00140139008927094>.
- [9] W. Lotens, Heat transfer from humans wearing clothing, Doctoral thesis TNO Institute for Perception, Soesterberg, The Netherlands, 1993.
- [10] K. Ghali, M. Othmani, B. Jreije, N. Ghaddar, Simplified heat transport model of a wind-permeable clothed cylinder subject to swinging motion, *Textil Res J* 79 (2009) 1043–1055, <http://dx.doi.org/10.1177/0040517508101460>.
- [11] N. Ghaddar, K. Ghali, M. Al-Othmani, I. Holmer, K. Kuklane, Experimental and theoretical study of ventilation and heat loss from isothermally heated clothed vertical cylinder in uniform flow field, *J Appl Mech* 77 (2010) 031011, <http://dx.doi.org/10.1115/1.4000429>.
- [12] N. Ismail, N. Ghaddar, K. Ghali, Predicting segmental and overall ventilation of ensembles using an integrated bioheat and clothed cylinder ventilation models, *Textil Res J* 84 (2014) 2198–2213, <http://dx.doi.org/10.1177/0040517514535868>.
- [13] N. Ghaddar, K. Ghali, B. Jones, Integrated human-clothing system model for estimating the effect of walking on clothing insulation, *Int J Therm Sci* 42 (2003) 605–619, [http://dx.doi.org/10.1016/s1290-0729\(03\)00026-7](http://dx.doi.org/10.1016/s1290-0729(03)00026-7).
- [14] K. Ghali, N. Ghaddar, B. Jones, Modeling of heat and moisture transport by periodic ventilation of thin cotton fibrous media, *Int J Heat Mass Tran* 45 (2002) 3703–3714, [http://dx.doi.org/10.1016/s0017-9310\(02\)00088-1](http://dx.doi.org/10.1016/s0017-9310(02)00088-1).
- [15] N. Ghaddar, K. Ghali, J. Harathani, Modulated air layer heat and moisture transport by ventilation and diffusion from clothing with open aperture, *J Heat Tran* 127 (287) (2005), <http://dx.doi.org/10.1115/1.1857949>.
- [16] N. Ismail, N. Ghaddar, K. Ghali, Determination of segmental and overall ventilation of clothed walking human by means of electric circuit analogy, *Textil Res J* 88 (2018), <http://dx.doi.org/10.1177/0040517516685284>.
- [17] M. Salloum, N. Ghaddar, K. Ghali, A new transient bioheat model of the human body and its integration to clothing models, *Int J Therm Sci* 46 (2007) 371–384, <http://dx.doi.org/10.1016/j.ijthermalsci.2006.06.017>.
- [18] G. Fu, A transient, 3-D mathematical thermal model for the clothed human, Ph.D. Thesis Kansas State University, Kansas, 1995.
- [19] N. Ghaddar, K. Ghali, S. Chehaitly, Assessing thermal comfort of active people in transitional spaces in presence of air movement, *Energy Build* 43 (2011) 2832–2842, <http://dx.doi.org/10.1016/j.enbuild.2011.06.040>.
- [20] N. Ghaddar, K. Ghali, M. Othmani, Effect of moisture transport on mixed convection in vertical annulus of a heated clothed vertical wet cylinder in uniform cross wind, 14th international heat transfer conference, vol. 7, 2010, pp. 215–223, <http://dx.doi.org/10.1115/ihtc14-22342>.
- [21] D. Ambesi, C.R. Kleijn, E.A. Hartog, R.H. Bouma, P. Brasser, Forced convection mass deposition and heat transfer onto a cylinder sheathed by protective garments, *AICHE J* 60 (2014) 353–361.
- [22] J. Lim, H. Choi, E.K. Roh, Assessment of airflow and microclimate for the running wear jacket with slits using CFD simulation, *Fash Textil* 2 (2015), <http://dx.doi.org/10.1186/s40691-014-0025-2>.
- [23] J. Werner, Man in extreme thermal environment — prediction based on a PC-model, *J Therm Biol* 18 (1993) 439–441.
- [24] T. Takemori, T. Nakajima, Y. Shoji, A fundamental model of the human thermal system for prediction of thermal comfort, *Trans Jpn Soc Mech Eng* 61 (1995) 1513–1520.
- [25] D. Fiala, K.J. Lomas, M. Stohrer, A computer model of human thermoregulation for a wide range of environmental conditions: the passive system, *J Appl Physiol* 87 (1999) 1957–1972.
- [26] D. Fiala, K.J. Lomas, M. Stohrer, Computer predictions of human thermoregulatory and temperature responses to a wide range of environment conditions, *Int J Biometeorol* 45 (2001) 143–159.
- [27] C. Huizenga, Z. Hui, E. Arens, A model of human physiology and comfort for assessing complex thermal environments, *Build Environ* 36 (2001) 691–699.
- [28] M. Salloum, N. Ghaddar, K. Ghali, A new transient bioheat model of the human body and its integration to clothing models, *Int J Therm Sci* 46 (2007) 371–384.
- [29] M. Al-Othmani, N. Ghaddar, K. Ghali, A multi-segmented human bioheat model for transient and asymmetric radiative environments, *Int J Heat Mass Tran* 51 (23–24) (2008) 5522–5533.
- [30] J. Werner, M. Buse, Temperature profiles with respect to inhomogeneity and geometry of the human body, *J Appl Physiol* 65 (1988) 1110–1118.
- [31] American Society for Testing and Materials, Standard test method for air permeability of textile fabrics, ASTM (1983) D737–D775 [IBR approved].
- [32] M. Jetté, K. Sidney, G. Blümchen, Metabolic equivalents (METS) in exercise testing, exercise prescription, and evaluation of functional capacity, *Clin Cardiol* 13 (1990) 555–565, <http://dx.doi.org/10.1002/clc.4960130809>.
- [33] Instruments for textile & biophysical testing brochure: Newton thermal manikin system, Advanced Thermal Measurement Technologies, Seattle, WA, USA, 2015 Thermetrics Inc.